Available online at www.sciencedirect.com
ScienceDirect
Journal of Molecular Catalysis A: Chemical 265 (2007) 283–291
JOURNAL OF MOLECULAR CATALYSIS A: CHEMICAL
www.elsevier.com/locate/molcata

Studies on the platinum and ruthenium nanoparticles catalysed reaction of aniline with 4-aminoantipyrine in aqueous and microheterogeneous media

J. Santhanalakshmi [a,*], J. Kasthuri [a], N. Rajendiran [b]

[a] *Department of Physical Chemistry, University of Madras, Guindy Campus, Chennai 600025, India*
[b] *Department of Polymer Science, University of Madras, Guindy Campus, Chennai 600025, India*

Received 5 April 2006; received in revised form 6 October 2006; accepted 10 October 2006
Available online 14 October 2006

Abstract

Platinum and ruthenium nanoparticles (Pnp, Rnp) are found to catalyse the dye formation reaction of aniline (AN) with 4-aminoantipyrine (AAP) in an acidic aqueous medium. The kinetic parameters of the reaction were studied by UV–vis spectroscopy. Pseudo first order kinetics and the total order equal to 2.0 are detected in both Pnp and Rnp systems. In the presence and absence of microheterogeneous media, the rate and order of the antipyrilquinoneimine dye formation depends on the nature of the metal nanoparticles, pH, ionic strength and different microheterogeneous media such as sodium dodecylsulfate (SDS), cetyltrimethylammonium bromide (CTAB) and tritonX-100 (TX-100). In the acidic medium, the catalytic effect of Rnp is found to be greater than that of Pnp. In the microheterogeneous medium, the optimized reaction rate of product formation follows the order SDS > TX-100 > CTAB. A possible reaction pathway has been proposed involving the activation of AN and AAP by metal nanoparticles and concomitant reactions of free radicals. Transmission electron microscopy (TEM) results show that the particle sizes are 12.0 nm and 7.0 nm, respectively, for Pnp and Rnp in the aqueous medium.

Keywords: Platinum nanoparticles; Ruthenium nanoparticles; Catalysis; Aniline; Microheterogeneous medium; Antipyrilquinoneimine dye

1. Introduction

Anilines (AN) are one of the widely distributed functional groups in the aquatic environment originating from the waste water discharges from dye, drug, polymer, and cosmetics manufacturing units and reductive degradation of cellular materials [1,2]. ANs constitute a highly toxic, potentially carcinogenic, slowly degrading, and eco-deadly family of chemicals [3,4]. Numerous different methods have been reported on the detection, analysis and removal of ANs from water and soil samples [5–7]. The enzymatic oxidation of aromatic amines plays a significant role in many biotransformation processes such as chemical carcinogenesis and drug metabolism. The oxidation of aromatic amines may lead to various products such as nitroso-, nitro-, azo-, and azoxy benzenes, etc. Various methods involving enzymes, metal chelates and H_2O_2 were employed in the earlier studies to detect and analyse ANs [8,9]. With analogous aim, the use of platinum and ruthenium nanoparticles (Pnp, Rnp) in an aqueous medium as catalysts on the reaction of AN (which is considered as a representative of aromatic amines) with 4-aminoantipyrine (AAP) has been attempted and presented in this paper. In the earlier studies, the same reaction of AN and phenol with AAP in the presence of H_2O_2 with catalyst such as a metal tetrasulfophthalocyanine is found to produce an intense pink colored water soluble dye product that can be precisely and easily detected and estimated by UV–vis spectroscopy [10,11].

The dye formation reaction between AN and AAP does not proceed without any catalysts and many reports exist on the effect of many different types of catalyst on this reaction. Pnp and Rnp in aqueous medium are of great interest due to their high surface area, stability and catalytic activity towards many reactions. The kinetics of the dye formation by AN and AAP is followed by UV–vis spectrophotometry. The coupling reaction of AN and AAP involves the formation of the [C_B=N–] group, where C_B is the benzene ring of AN and N belongs to the amino group of AAP molecules, respectively. The characteristic FT-IR peaks are found at 1627 cm^{-1} for Pnp and 1635 cm^{-1} for Rnp systems, respectively. The reaction conditions are optimized by

* Corresponding author. Tel.: +91 44 22351137x228.
E-mail address: nrajendiar@yahoo.com (N. Rajendiran).

1381-1169/$ – see front matter © 2006 Published by Elsevier B.V.
doi:10.1016/j.molcata.2006.10.012

investigating the effects of AN, AAP, Pnp, Rnp, ionic strength and pH on the kinetics of the reaction. The kinetic parameters are determined by using UV–vis spectroscopy. Addition of cationic, anionic and non-ionic surfactants in solution alters the rates of the dye formation reaction between AN and AAP and other related reactions when carried out in the presence of different catalysts. Earlier reports exist on the oxidation of aromatic amines in the presence of surfactant micelles [12]. The effect of microheterogeneous media on the dye formation reaction in the presence of Pnp and Rnp will be new and interesting. The results clarify the interactions of AN with Pnp and Rnp and their role in the reaction pathway of the dye formation reaction in water.

2. Experimental

2.1. Reagents and instruments

Aniline, 4-aminoantipyrine, hexachloroplatinic acid hexahydrate, polyvinyl pyrrolidone, and ruthenium trichloride trihydrate were purchased from Aldrich and were used as such. Ethylene glycol is an analytical grade reagent, Loba-Chemie India Ltd. Deionised and double distilled water in all glass assembly was used to prepare aqueous solutions. All other chemicals, KNO_3, buffers, surfactants belong to the analytical grade with highest purity ca. 99.9%. UV–vis spectroscopic measurements were performed on a Schimadzu UV-1601 double beam instrument. The optical length of the quartz cuvette is 1 cm.

2.2. Preparation of platinum and ruthenium nanoparticles in aqueous medium

The metal nano colloids were prepared in a four-necked round bottom flask following the reported procedure with small modifications [13]. There are several reports available on Pnp and Rnp preparation [14,15]. Poly(vinylpyrrolidone) (PVP) (30 mg) was dissolved in 10 ml of ethylene glycol (EG) at room temperature under constant stirring. 50 mg of hexachloroplatinic acid hexahydrate ($H_2PtCl_6{\cdot}6H_2O$) was dissolved in 5 ml of EG separately, and both solutions were heated up to 150 °C at the rate of 5 °C/min. Into the reaction flask, H_2PtCl_6–EG and PVP–EG solutions were added dropwise with constant stirring and maintaining the high temperature. The addition of EG solutions was completed by 20 min and the reaction was stopped after 1 h duration. The contents in the flask were initially pale yellow and turns to dark honey colored transparent solution, which indicates the completion of nano colloid formation. The stability of the colloidal dispersion was ascertained by maintaining −5 °C in a cryostat for 1 h. In the case of ruthenium nano colloid, 11 mg ruthenium trichloride trihydrate ($RuCl_3{\cdot}3H_2O$) was dissolved in 5 ml of EG and added with 250 mg of PVP dissolved in 20 ml of EG. The mixture was heated up to 150 °C with constant stirring. Dark honey colored solution confirmed the formation of ruthenium nanoparticles. All the reactions with nanoparticles were conducted at room temperature.

2.3. Size determination by TEM

Transmission electron microscopy (TEM) measurements were conducted by placing a small drop of particle suspension on a formvar coated copper grid and allowed to evaporate very slowly in vacuum under ambient temperature. The TEM photographs were taken on a JEOL model 1200 EX instrument operated at an accelerating voltage of 120 kV [16].

2.4. Product identification and characterization

The concentrations of AN solutions were checked spectroscopically from the absorbance values at $\lambda_{max} = 280$ nm with $\varepsilon = 1.2 \times 10^3\ cm^{-1}\ M^{-1}$ [17]. The reactions were carried out in a two-necked flask initially containing AN and AAP aqueous solutions with constant stirring kept in a thermostat at 25 °C. The dye formation reaction occurred only on addition of Pnp or Rnp. Hence, time of addition of Pnp or Rnp was taken as the time of initiation of the reaction. Kinetics was followed by the absorbance changes of an aliquot of the reaction mixture at regular intervals of time at constant $\lambda_{max} = 532$ nm for both Pnp and Rnp systems. The λ_{max} values correspond to the dye product. The disappearance of the characteristic absorption peak of the reactants (AN and AAP) in the reaction mixture ensured the completion of the reaction. FT-IR spectra of the dye formed between AN and AAP in the presence of Rnp and Pnp were recorded in KBr disks at 25 °C from 500 cm^{-1} to 4000 cm^{-1} using a Perkin-Elmer FT-IR instrument. The IR peaks of the Rnp catalysed dye product are more intense than those of the Pnp catalysed product.

2.5. Cyclic voltammetry

Cyclic voltammograms of the aqueous solutions of reactants containing Pnp and Rnp were obtained using EG&G Instruments PAR 283 potentiostat/galvanostat. A conventional three-electrode electrochemical cell was used with a coiled, platinised Pt wire as the counter electrode and Ag/AgCl in 3 M HCl as the reference. The supporting electrolyte was 0.5 M H_2SO_4. The working electrode was a Pt disk (2 mm × 5 mm), which was cleaned, flame treated and cooled in air after each measurement. The scan rate was fixed at 25 mV/s. All the measurements were carried out at 25 °C [18].

3. Results and discussion

3.1. Kinetic studies from spectral data

Fig. 1 shows the typical UV–vis spectra of AN, AAP and the dye formed in aqueous solution when the reactants are mixed in the presence of Pnp and Rnp catalytic systems at 25 °C. Since the dye formation reaction takes place only when nanoparticles are added, peaks found at 532 nm for both Pnp and Rnp catalysed systems are considered to be characteristic of the dye product. The growth of the absorbance of the peak with time is proportionate to the rate of dye formation. In Fig. 2, UV–vis spectra at various reaction times are given. The effects of compositional

Table 1
The pseudo first order rate coefficient of Pnp catalysed dye formation reaction between AAP and AN in aqueous media at 25 °C

Serial number	Symbols[a]	[AN] ($\times 10^{-2}$ M)	[AAP] ($\times 10^{-2}$ M)	[KNO_3] ($\times 10^{-1}$ M)	pH	[Pnp] ($\times 10^{-4}$ M)	k ($\times 10^{-2}$ s^{-1})
1	△	3.35	2.67	–	3.2	2.94	1.84
2	□	3.35	3.35	–	3.2	2.94	2.17
3	■	2.67	3.35	–	3.2	2.94	1.69
4	×	3.35	3.35	–	3.2	4.52	2.34
5	♦	3.35	3.35	–	3.2	5.86	2.56
6	◊	3.35	3.35	2.03	3.2	2.94	2.72
7	●	3.35	3.35	–	2.6	2.94	1.43
8	○	3.35	3.35	–	3.6	2.94	2.28
9	✱	3.35	3.35	–	4.4	2.94	1.31
10	▲	3.35	3.35	–	5.4	2.94	1.05

[a] These symbols are used in the figures.

variations in AN, AAP, Pnp, Rnp, salt and pH on the absorbance-time dependence are given in Fig. 3. The exact compositions are shown in Table 1, corresponding to the respective serial numbers assigned to each of the reaction mixture. In Fig. 4, the kinetic plots of log X against time, where $X = [(OD_\alpha)/(OD_\alpha - OD_t)]$ and OD_t and OD_α refer to absorbances at time 't' and at completion of reaction are given. Completion of reaction is ensured when absorbance remains unchanged with further increase in time. These plots are used to determine the rate coefficients of the dye formation reaction under different experimental conditions.

In Tables 1 and 2, the rate coefficient values are given for the Pnp and Rnp catalytic systems. For Rnp catalysed systems it may be seen that comparatively lower concentration of AN, AAP are sufficient to bring about a similar rate constant value as that of Pnp catalysed systems. In the effects of pH and ionic strength for Rnp systems at lower compositions of AN and AAP higher rate coefficient values are detected. That is, when the concentration of the reactants, pH and ionic strength of the medium are the same, higher rates are attained in the Rnp catalytic systems than in the Pnp ones. Although the optimum pH for maximum rate values are different for the Rnp and Pnp catalytic systems, the maximum rate found in the Rnp catalysed system is greater than that found in the Pnp one. Based on the compositional effects of AN and AAP and adopting pseudo first order conditions, the order with respect to each of the reactants is found to be 1.0 and the total order 2.0. This is observed in both the Pnp and Rnp catalysed systems. The rate coefficient values correspond to the pseudo first order rate constant of the reactions. The catalyst concentration in Rnp system is nearly ten times lower than the concentration of Pnp. This indicates that Rnp shows a higher catalytic activity than Pnp in this reaction.

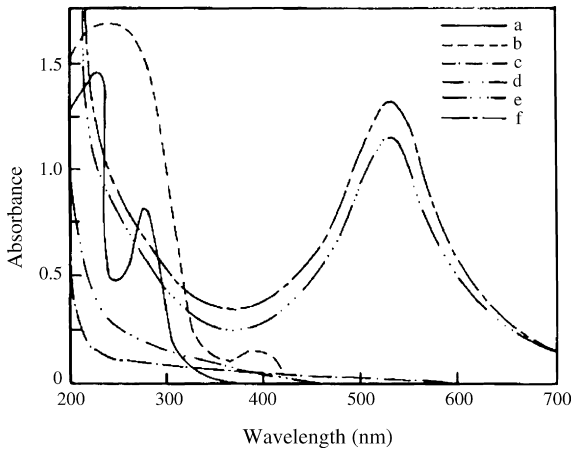

Fig. 1. Typical UV–vis spectra of (a) AN (3.35×10^{-2} M), (b) 4-aminoantipyrine (AAP) (3.35×10^{-2} M), (c) platinum nanoparticles (Pnp) (2.94×10^{-4} M), (d) ruthenium nanoparticles (Rnp) (1.78×10^{-5} M), (e) dye in the presence of Pnp ($\lambda_{max} = 532$ nm) and (f) dye in the presence of Rnp ($\lambda_{max} = 532$ nm) in aqueous medium at 25 °C.

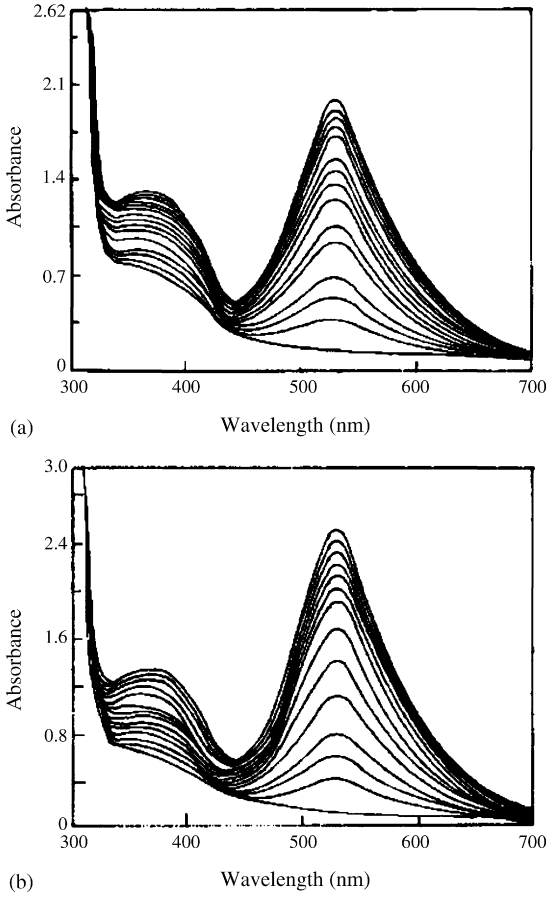

Fig. 2. UV–vis spectra of the dye formation reaction between AN and AAP at various times in aqueous media at 25 °C in the presence of (a) Pnp and (b) Rnp. [AN] = [AAP] = 3.35×10^{-2} M; [Pnp] = 2.94×10^{-4} M; [Rnp] = 1.78×10^{-5} M.

Table 2
The pseudo first order rate coefficient of Rnp catalysed dye formation reaction between AAP and AN in aqueous media at 25 °C

Serial number	Symbols[a]	[AN] ($\times 10^{-3}$ M)	[AAP] ($\times 10^{-3}$ M)	[KNO_3] ($\times 10^{-1}$ M)	pH	[Rnp] ($\times 10^{-5}$ M)	k ($\times 10^{-2}$ s^{-1})
1	△	5.61	5.61	–	4.0	1.78	2.30
2	□	5.61	4.37	–	4.0	1.78	2.05
3	■	4.37	5.61	–	4.0	1.78	1.82
4	×	5.61	5.61	–	4.0	2.15	2.58
5	♦	5.61	5.61	–	4.0	1.24	1.56
6	◊	5.61	5.61	2.45	4.0	1.78	2.89
7	●	5.61	5.61	–	2.6	1.78	1.62
8	○	5.61	5.61	–	3.6	1.78	2.40
9	✱	5.61	5.61	–	4.4	1.78	2.65
10	▲	5.61	5.61	–	5.4	1.78	1.38

[a] These symbols are used in the figures.

3.2. Effect of variations in catalyst

Although Pnp and Rnp are synthesized under similar conditions, the catalytic activity of Pnp is different from Rnp since particle sizes of these systems differ very much [19,20]. Tables 1 and 2 show that the presence of Pnp or Rnp initiates the dye formation reaction with appreciable rate coefficients. On increasing the concentration of Pnp (serial nos. 2, 4, 5) the rate coefficient increases for constant compositions of AN and AAP. The increase in the concentration of Rnp also results in increase in the rate of the reaction (Table 2, serial nos. 1, 4, 5). This effect is similar to the Pnp system. In Table 1, it is seen that the catalyst concentrations in no. 8 is lower than systems in nos. 4 and 5. But the pH is higher (3.6) than that of the serial nos. 4 and 5. The optimum pH for the maximum rate is equal to 3.6 for Pnp systems and 4.4 for Rnp systems, respectively.

3.3. Effect of salt

Addition of inert electrolyte to an ion–ion reaction alters the rate coefficient depending on the nature of the charge of the reactants. In the present study AN and AAP are neutral and no change in the rate coefficient values is expected in the presence of electrolytes. However, in the presence of KNO_3, while the compositions of AN, AAP and Pnp are kept constant, the rate coefficient increases (Table 1, no. 6). The color of the dye

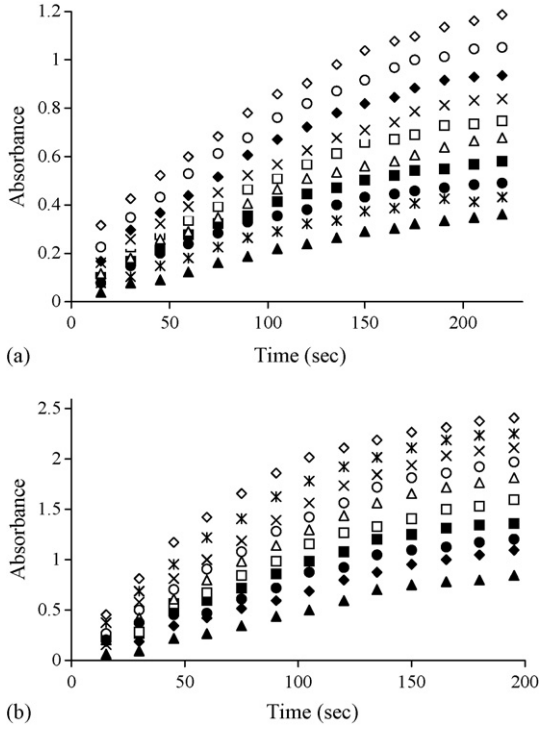

Fig. 3. Absorbance vs. time plots for the dye formation reaction between AN and AAP in the presence of (a) Pnp and (b) Rnp in aqueous media at 25 °C under various experimental conditions. λ_{max} of the absorbance values: (a) 532 nm and (b) 532 nm. The compositions of the reaction mixtures are given in Table 1 for the Pnp system and in Table 2 for the Rnp one as follows: 1 (△); 2 (□); 3 (■); 4 (×); 5 (♦); 6 (◊); 7 (●); 8 (○); 9 (✱); 10 (▲).

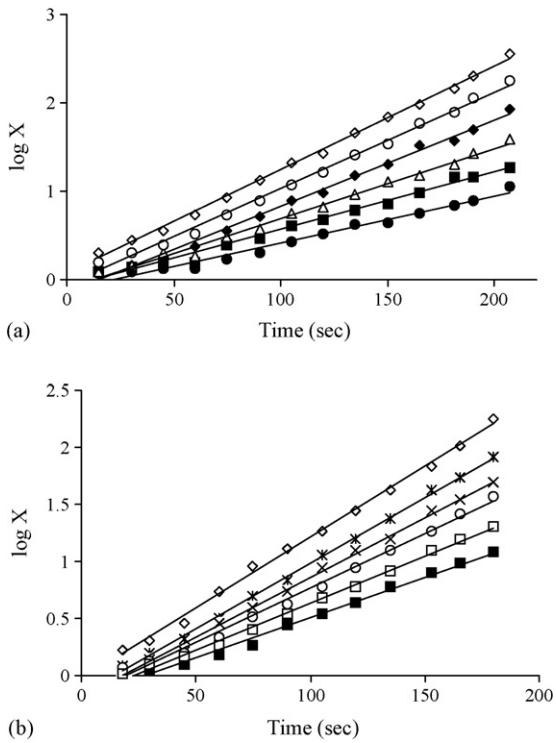

Fig. 4. Kinetic plots of the dye formation reaction between AN and AAP in the presence of (a) Pnp and (b) Rnp in aqueous media at 25 °C under various experimental conditions. The compositions of the reaction mixture are the same as those given in Table 1 for Pnp and Table 2 for Rnp, respectively. The serial nos. are: 1 (△); 2 (□); 3 (■); 4 (×); 5 (♦); 6 (◊); 7 (●); 8 (○); 9 (✱).

formed in the presence of electrolyte is more intense than in the absence of the electrolyte. The positive effect of ionic strength on the rate coefficient of the reaction indicates that both the reactants are similarly charged in the pH controlled medium [21]. For both Pnp and Rnp systems, acidic pH medium is used in which AN and AAP exist in the protonated form. In similarly charged conditions of AN and AAP the overall rate increases in the presence of electrolyte. The catalytic activity of Pnp and Rnp is considered to the activation of AN to react with AAP and vice versa. In the case of Rnp (Table 2, no. 6) a similar increase in the rate coefficient is seen in the presence of KNO_3. The extent of increase in the rate coefficient is found higher in Rnp than in Pnp.

3.4. Effect of pH

When the medium is changed to basic conditions, the reaction does not proceed at all and no coloration of the dye is found. In the acidic medium, the optimum pH with the maximum rate coefficient was found to be 4.4 for the Rnp system and 3.6 for the Pnp system, respectively. The dye formation reaction is pH sensitive. The pH profiles are shown in Fig. 2a and b for Pnp and Rnp systems, respectively. The rate coefficient found in the Rnp catalysed system is higher than in the Pnp catalysed system. In the acidic medium, AN is protonated to anilinium ion in which the para position is activated [22,23]. Further reaction with AAP at the para position leads to the dye formation.

Table 3
Characteristic wavelength maxima of the dye product of the AN + AAP reaction with Pnp and Rnp in the presence of various surfactants in aqueous solution at 25 °C

Serial number	Surfactant	Pnp λ_{max} (nm)	Rnp λ_{max} (nm)
1	SDS	534	535
2	TX-100	533	533
3	CTAB	532	532

3.5. Effect of microheterogeneous media

The dye formation reactions in the presence of Pnp and Rnp seem to be affected by the presence of surfactant micelles in solution. This effect is possibly attributed to the hydrophobic interactions of SDS (anionic), CTAB (cationic) and TX-100 (non-ionic) micelles either with substrates or with reactive intermediates of Pnp or Rnp particles. Table 3 shows the changes in λ_{max} of the dye formed in the presence of various micelles in solution. Only marginal shift in λ_{max} are seen. Fig. 5 demonstrates the effect of microheterogeneous media on the absorbance versus time plots in the presence of Pnp and Rnp. The corresponding kinetic plots used for the rate coefficient determination is given in Fig. 6. The values of rate coefficient in the presence of various surfactant micelles are presented in Table 4. Here the SDS system shows a higher rate coefficient value than other surfactant systems.

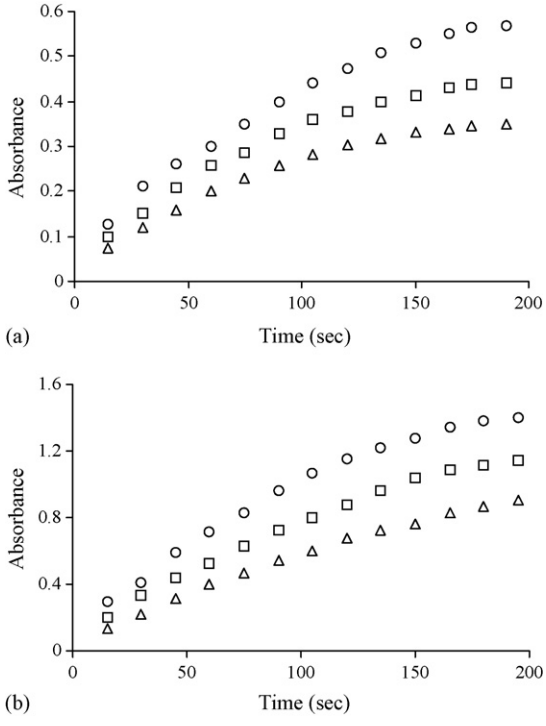

Fig. 5. Absorbance vs. time plots of the dye formation reaction between AN and AAP in the presence of (a) Pnp and (b) Rnp in various aqueous microheterogeneous media at 25 °C. [TX-100] = 10% (w/v); [SDS] = [CTAB] = 0.01 M; [AAP] = [AN] = 3.35×10^{-2} M; [Pnp] = 2.94×10^{-4} M; [Rnp] = 1.78×10^{-5} M. The serial nos. are as follows: (1) SDS (◯), (2) TX-100 (□), and (3) CTAB (△).

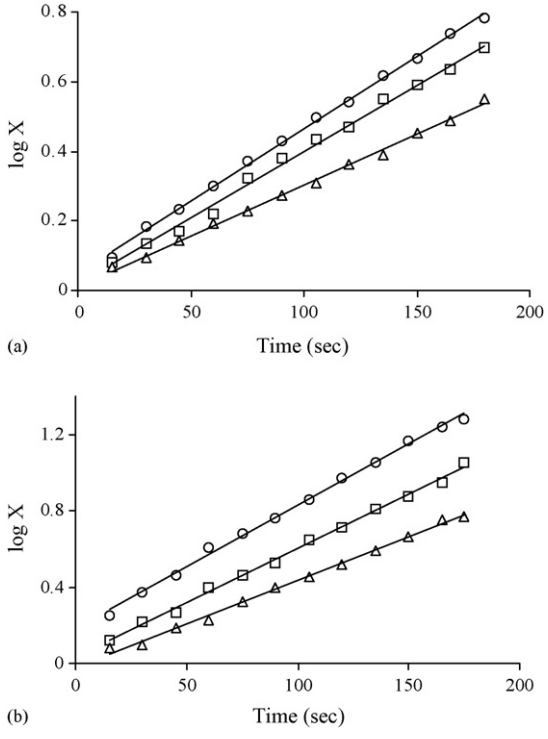

Fig. 6. Kinetic plots of the dye formation reaction between AN and AAP in the presence of different aqueous microheterogeneous media containing (a) Pnp and (b) Rnp. [TX-100] = 10% (w/v); [SDS] = [CTAB] = 0.01 M; [AAP] = [AN] = 3.35×10^{-2} M; [Pnp] = 2.94×10^{-4} M; [Rnp] = 1.78×10^{-5} M. The serial nos. are as follows: (1) SDS (◯), (2) TX-100 (□), and (3) CTAB (△).

Table 4
Rate coefficient (s^{-1}) of the dye formation reaction between AAP and AN in the presence of microheterogeneous media catalysed by Pnp and Rnp, respectively, at 25 °C

Serial number	System	Symbols	Pnp k ($\times 10^{-3}\ s^{-1}$)	Rnp k ($\times 10^{-2}\ s^{-1}$)
1	SDS	○	9.57	1.48
2	TX-100	□	8.85	1.31
3	CTAB	△	6.74	1.04

[Pnp] = 2.94×10^{-4} M; [Rnp] = 1.78×10^{-5} M; [TX-100] = 10% (w/v); [SDS] = [CTAB] = 0.01 M; [AAP] = [AN] = 3.35×10^{-2} M.

It is seen that in the presence of microheterogeneous media the rate coefficient in the Rnp catalytic system is greater than in the Pnp one. For both Rnp and Pnp the rate coefficients are found in the following order: SDS > TX-100 > CTAB. The anionic surfactant SDS seems to interact well with the Pnp and Rnp particulates and enhances the stability of the intermediates adsorbed on the particulates [24]. In acidic media, anionic micelles interact better with the protonated forms of AN and AAP than the TX-100 and CTAB systems. CTAB micelles being cationic, its interaction with protonated AN and AAP will be weaker than in the SDS system [25,26]. TX-100 micelles being neutral, the effect of TX-100 on the rate coefficient of the reaction lies in between SDS and CTAB.

When the rate coefficients values of the reactions carried out in the absence and in the presence of microheterogeneous media are compared it is found that the presence of micelles lowers the rate coefficient. These effects could be due to the partitioning of the reactive substrate between the nanoparticles and the micelles or to the micelles intercalating with the capping material (polyvinyl pyrrolidone) of the particles.

3.6. FT-IR spectral studies

In Fig. 7, the FT-IR spectra of the antipyrilquinoneimine dye formed in the presence of Pnp and Rnp systems are presented. In the Rnp system, intensity of the peaks are higher; the 1635 cm^{-1} peak characteristic of [C_B=N–], where C_B refers to benzene ring carbon Scheme 1 has been found to be more intense than in the Pnp catalysed dye product. This result is in agreement with the results from pH and salt effects.

Fig. 8 shows the TEM photographs of pure Pnp and Rnp system. In the case of Pnp and Rnp the average particle sizes

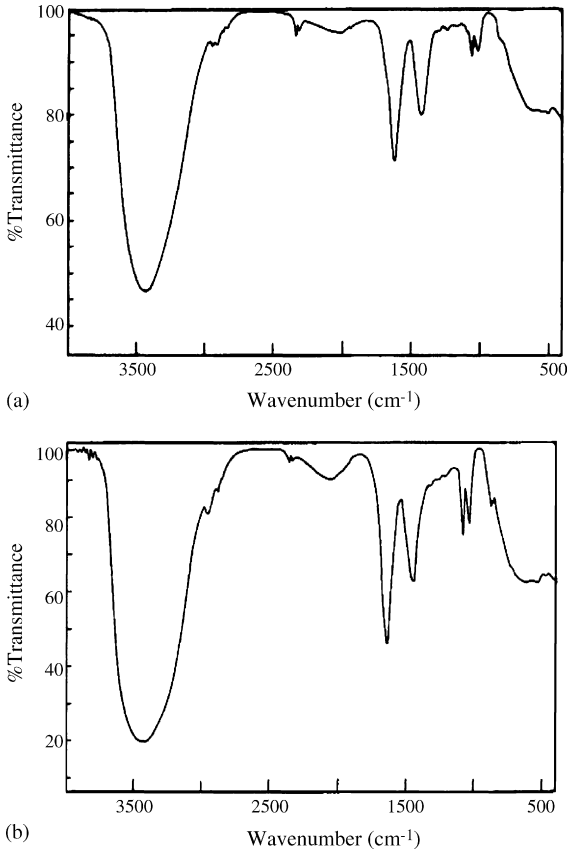

Fig. 7. FT-IR spectra of the AN–AAP dye containing (a) Pnp and (b) Rnp systems taken in KBr disc at 25 °C.

fall in the range of 12.0–7.0 nm, respectively. In both the cases, spherical particles are observed. Due to the smaller size, a greater number of particles is found in Rnp, which is consistent with its higher catalytic activity. Rnp is found to exhibit narrower dispersity in particle sizes than Pnp.

3.7. Cyclic voltammetry (CV) studies

The cyclic voltammograms of pure Pnp, Rnp with AAP and AN, at various times are given in Fig. 9. Pt versus Ag/AgCl reference electrode is used as the working electrode. The supporting electrolyte is 0.5 M H_2SO_4. The peaks are observed at 0.45 V and 0.43 V, respectively, for pure Pnp and Rnp [27]. On addition of reactants the new peaks at 0.65 V and 0.62 V appear

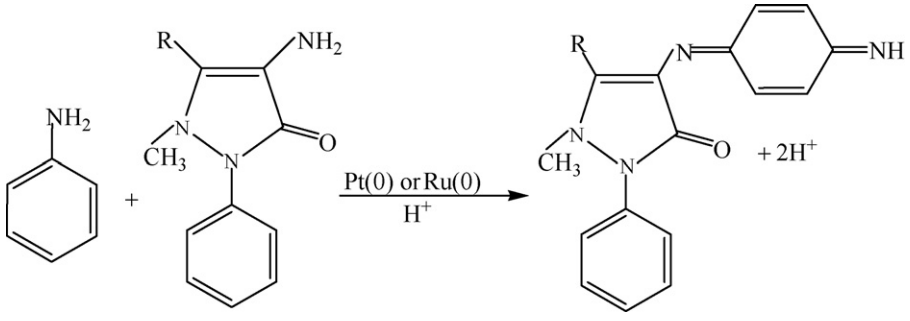

Scheme 1.

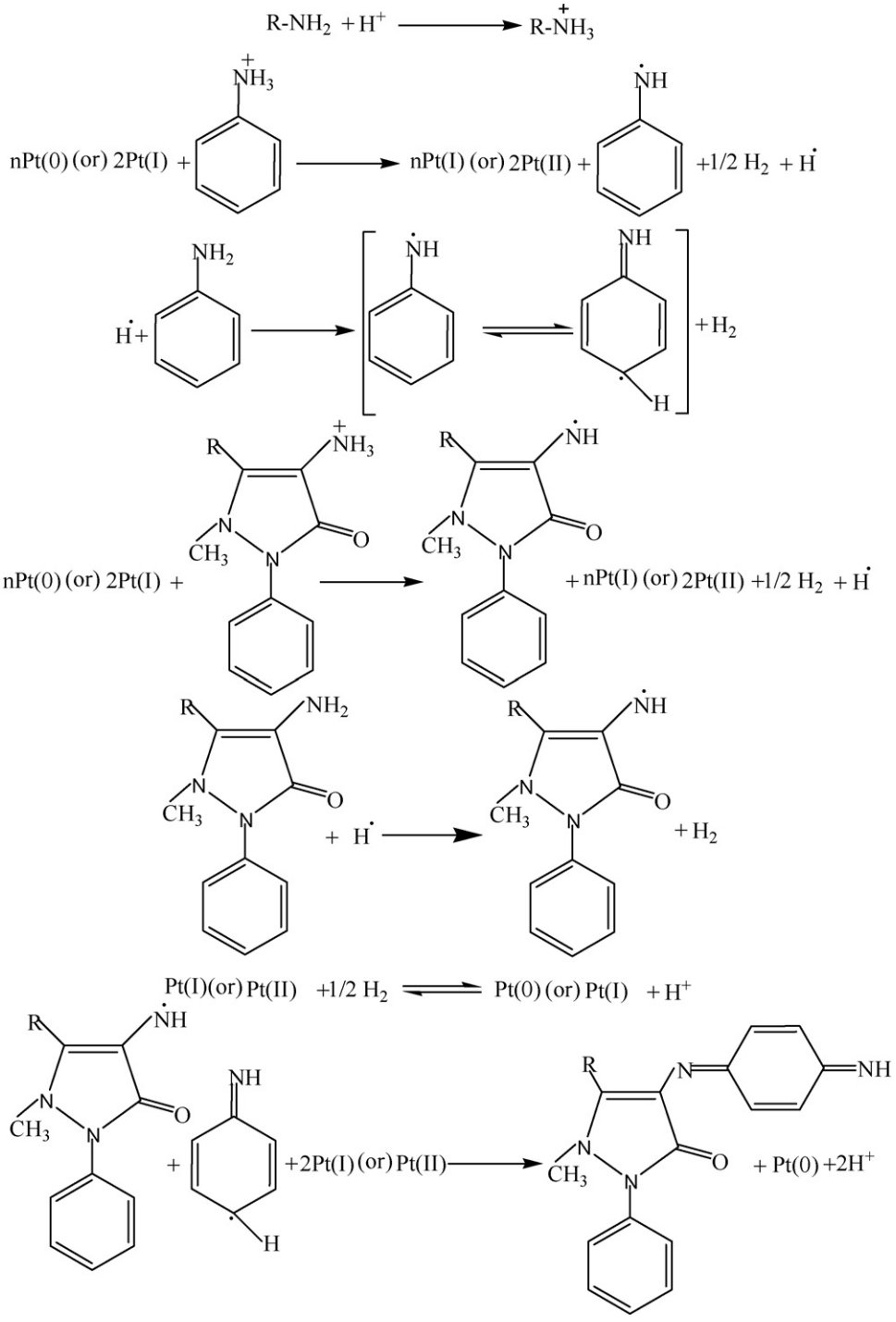

Scheme 2.

for Pnp and Rnp systems, respectively. This ensures the binding of all of Pnp with AN and AAP. As the time of the reaction progresses the intensity (I_p) of the peak characteristic of the dye increases tremendously. For both Rnp and Pnp systems, during the dye formation the peak potential values are found to be nearly constant. For nanoparticulate catalytic systems, CV provides a potential tool to study the electrochemical kinetics of the dye formation [28]. Also in the Rnp system the cyclic voltammograms are more prominent than in the Pnp one. Similar results are also obtained in kinetic studies.

3.8. Reaction pathway

In acidic pH the protonated form of the amines exist in equilibrium with the non-protonated species. Both AN and AAP exist in such an equilibrium in the acidic medium (Scheme 1). When Pnp is added to AN and AAP mixed in acidic solutions, $H^{\bullet}$ radical tagged AAP and AN are found with the generation of Pt(I) or Pt(II), which is represented in Scheme 2. The dye formation reaction is initiated by Pt(I) or Pt(II) which generates Pt(0) back into the medium. The neutral, non-protonated forms

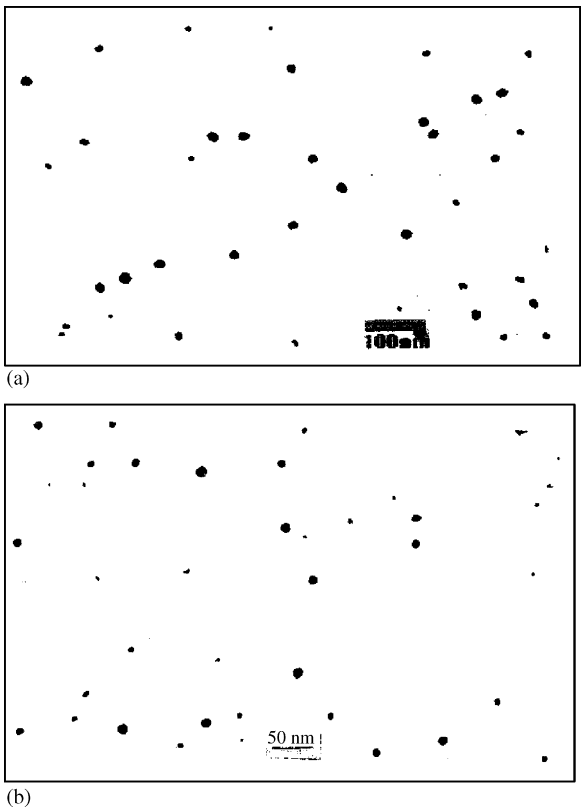

Fig. 8. Transmission electron microphotographs of (a) Pnp and (b) Rnp on formvar coated copper grids.

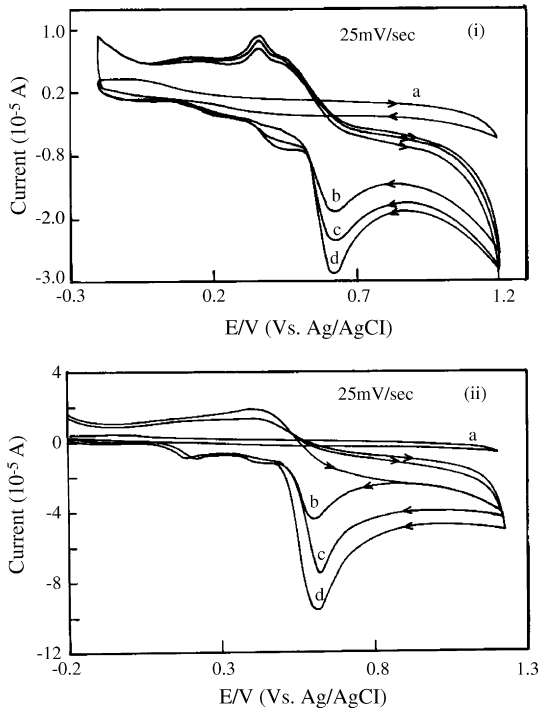

Fig. 9. Cyclic voltammograms of the dye formation between AN and AAP at 25 °C using Pt working electrode vs. Ag/AgCl reference electrode. Supporting electrolyte: 0.5 M H_2SO_4. (i) a, Pnp; b, Pnp + reactants at 3 min; c, at 5 min; d, at 15 min. (ii) a, Rnp, b, Rnp + reactants at 3 min; c, at 5 min; d, at 15 min.

of AN and AAP are activated by $H^{\bullet}$ radicals. A similar mechanism can be put forth for Rnp involving AN and AAP in the acidic medium.

As a spot test, the presence of radicals during the reaction course was tested by the addition of a few drops of acrylonitrile monomer. Soon after the addition the solution turns turbid due to the white polymer product formed which is subsequently precipitated. The generation of Pt(0) or Ru(0) back into the reaction medium during the dye formation step is the versatile aspect of these reactions and ensures many turnovers of the Pnp and Rnp catalysts.

4. Conclusions

Pnp and Rnp prepared in this work have the sizes in the range of 12.0–7.0 nm when examined by TEM. Pnp and Rnp catalyse the dye reaction between AAP and AN in aqueous solutions. This reaction does not proceed in the absence of nanoparticles and in basic pH. The spectral characterization of the dye molecule agrees well with the literature. The kinetics follows the pseudo first order. Effects of pH, salt, catalysts and microheterogeneous media are studied. The optimum pH for the maximum rate is found to be 3.6 and 4.4 in the Pnp and Rnp catalytic systems, respectively. In both cases, the presence of microheterogeneous media lowers the rate coefficient in the following order: SDS > TX-100 > CTAB. Generally the Rnp system exhibits the higher rate coefficient than the Pnp one irrespective of the reaction medium. A general reaction pathway involving free radicals has been put forth to rationalize the observed results. This reaction may serve as a spot test to detect and analyse the composition of aniline in aqueous solutions using a spectrophotometry technique.

References

[1] Aromatic Amines: An Assessment of the Biological and Environmental Effects, Committee on Amines, Board of Toxicological and Environmental Health Hazards, Assembly of Life Sciences, National Research Council, 1981.
[2] E.M. Ward, G. Sabbioni, D.G. Debord, A.W. Teass, K.K. Brown, G.G. Talaska, D.R. Roberts, A.M. Ruder, P.R. Streicher, J. Natl. Cancer Inst. 88 (1996) 1046.
[3] H. Kataoka, J. Chromatogr. A 773 (1996) 19.
[4] L.S. Debruin, J.B. Pawliszyn, P.D. Josephy, Chem. Res. Toxicol. 12 (1999) 78.
[5] S. Premsingh, N.S. Venkataramanan, S. Rajagopal, S.P. Mirza, M. Vairamani, P.S. Rao, K. Velavan, Inorg. Chem. 43 (2004) 5744.
[6] E.H. Seymour, N.S. Lawrence, E.L. Beckett, J. Davis, R.G. Compton, Talanta 57 (2002) 233.
[7] A.D. Gunatilleka, C.F. Poole, Anal. Commun. 36 (1999) 325.
[8] K. Zhang, R.X. Cai, D.H. Chen, L.Y. Mao, Anal. Chim. Acta 413 (2000) 109.
[9] Q.L. Wang, Z.H. Liu, R.X. Cai, G.X. Lu, J. Anal. Chem. 30 (2002) 928.
[10] N. Rajendiran, J. Santhanalakshmi, J. Mol. Catal. A: Chem. 245 (2006) 185.
[11] E. Brillas, E. Mur, R. Sauleda, L. Sanchez, J. Peral, X. Domenech, J. Casado, Appl. Catal. B: Environ. 16 (1998) 31.
[12] H. Firouzabadi, N. Iranpoor, K. Amani, Green Chem. 3 (2001) 131.
[13] F. Bonet, V. Delmas, S. Grugeon, R.H. Orbina, P.-Y. Silvert, K.T. Elhsissen, Nanostruct. Mater. 11 (1999) 1277.
[14] J. Yang, T.C. Deivaraj, H.-P. Too, J.Y. Lee, Langmuir 20 (2004) 4241.

[15] T. Fujimoto, Y. Mizukoshi, Y. Nagata, Y. Maeda, R. Oshima, Scripta Mater. 44 (2001) 2183.
[16] C. Burda, X. Chen, R. Narayanan, M.A.E.I. Sayed, Chem. Rev. 105 (2005) 1025.
[17] C.N. Banwell, E.M. Mccash, Fundamental of Molecular Spectroscopy, 4th ed., TMH Publishing Company Ltd., New Delhi, 2000.
[18] H.A. Andeas, V.I. Birss, J. Phys. Chem. B 109 (2005) 3743.
[19] Y. Tan, X. Dai, Y. Fangli, D. Zhu, J. Mater. Chem. 13 (2003) 1069.
[20] A. Miyazaki, I. Balint, Y. Nakano, J. Nanoparticle Res. 5 (2003) 69.
[21] T. Herricks, J. Chen, Y. Xia, Nano Lett. 4 (2004) 2367.
[22] F. Fant, A. De Sloovere, K. Matthijsen, C. Marle, S. El Fantroussi, W. Verstraete, Environ. Pollut. 111 (2001) 503.
[23] H. Sajiki, T. Lkawa, K. Hirota, Org. Lett. 6 (2004) 4977.
[24] R.P. Bonar-Law, J. Org. Chem. 61 (1996) 3623.
[25] J. Tanori, M.P. Pileni, Langmuir 13 (1997) 639.
[26] I. Lisiecki, M. Borjling, L. Motte, B.W. Ninham, M.P. Pileni, Langmuir 11 (1995) 2385.
[27] Q. Lu, B. Yang, L. Zhuang, J. Lu, J. Phys. Chem. B 109 (2005) 1715.
[28] P. Waszczuk, J. Solla-Gullon, H.S. Kim, Y.Y. Tong, V. Montiel, A. Aldaz, Wieckowski, J. Catal. 203 (2001) 1.